

Abstract

A surface to bottom North-East Atlantic Ocean budget for mass, nutrients (nitrate and phosphate) and oxygen is determined using an optimization method based on climatological data from the World Ocean Atlas 2009 and three surveys of the OVIDE transect (from Greenland to Portugal). Budgets are derived for two communicating boxes representing the North Eastern European Basin (NEEB) and the Irminger Sea.

For the NEEB (Irminger) box, it is found that 30 % of the mass import (export) across the OVIDE section reach (originate from) the Nordic Seas while 70 % is redistributed between both boxes through the Reykjanes Ridge ($9.3 \pm 0.7 \times 10^9 \text{ kg s}^{-1}$).

Net biological source/sink terms of nitrate point to both the Irminger and NEEB boxes as net organic matter production sites (consuming nitrate at a rate of $-7.8 \pm 6.5 \text{ kmol s}^{-1}$ and $-8.4 \pm 6.6 \text{ kmol s}^{-1}$ respectively). Using a standard Redfield ratio of C:N = 106:16, nitrate consumption rates indicate that about 40 TgC yr^{-1} of carbon is fixed by organic matter production between the OVIDE transect and the Greenland-Scotland Ridge. Nutrients fluxes also induce a net biological production of oxygen of $73 \pm 60 \text{ kmol s}^{-1}$ and $79 \pm 62 \text{ kmol s}^{-1}$ in the Irminger and NEEB boxes which points to the region as being autotrophic.

Air-sea oxygen fluxes show an oceanic oxygen uptake in the two regions ($264 \pm 66 \text{ kmol s}^{-1}$ in the north and $443 \pm 70 \text{ kmol s}^{-1}$ in the south), dominated by the abiotic component. The abiotic flux is partitionned into a mixing and a thermal components. It is found that the Irminger Sea oceanic oxygen uptake is driven by an air-sea heat flux cooling increasing the ocean surface oxygen solubility. Over the North Eastern European Basin the mixing component is about half the thermal flux, presumably because of the oxygen minimum in the subtropical thermocline.

BGD

9, 4323–4360, 2012

Nutrients and oxygen budgets in the North-East Atlantic

G. Maze et al.

Title Page

Abstract

Introduction

Conclusions

References

Tables

Figures

⏪

⏩

◀

▶

Back

Close

Full Screen / Esc

Printer-friendly Version

Interactive Discussion

1 Introduction

The North-East Atlantic is a region where subtropical thermocline waters are carried in by the North Atlantic Current (NAC). Those water masses experience strong air-sea interactions and mixing and then either spread toward the Nordic Seas or recirculate westward to the Labrador Sea in the remaining of the subpolar gyre (see Fig. 1 in Schott et al., 2004). This surface circulation takes place on top of a deeper one characterized by (i) the mid-depth circulation of Labrador Sea water (Yashayaev et al., 2007; Kvaleberg et al., 2008) and (ii) the southward flow along the flanks of high topographic features – East Greenland shelf and Reykjanes Ridge – of the dense water masses primarily formed in the Nordic Seas and penetrating the North-East Atlantic through the sills between Greenland and Scotland (see Eldevik et al., 2009, and references therein). Intense vertical mixing occurs in winter in the Iceland Basin which results in the formation of subpolar mode waters (Brambilla and Talley, 2008; Brambilla et al., 2008; Thierry et al., 2008; de Boisséson et al., 2010, 2012). Moreover, the Irminger Sea is increasingly thought to be a region of periodic deep convection and mode water formation (Pickart et al., 2003a,b; Yashayaev, 2007; Falina et al., 2007; Sproson et al., 2008; Van Aken et al., 2011). The North-East Atlantic is thus a key horizontal and vertical crossroads region where strong air-sea interactions are at the origin of part of the deep water masses feeding the lower branch of the meridional overturning circulation.

However most of the attention has been toward the circulation of mass, heat and salt while basic nutrients and oxygen fluxes are still poorly constrained by observations in the region. One noticeable exception is the study by Álvarez et al. (2002) who derived a nitrate/nitrogen and oxygen budget for the North-East Atlantic region, north of the WOCE A25 4× section between Greenland and Portugal. But their transport estimates have been improved (Lherminier et al., 2007) so that their budgets have to be revisited, which will be done in this study. Oceanic nutrients and oxygen fluxes are useful quantities to improve our comprehension of the global carbon cycle. On one hand oceanic anthropic carbon fluxes and storage are determined knowing the natural carbon fluxes,

BGD

9, 4323–4360, 2012

Nutrients and oxygen budgets in the North-East Atlantic

G. Maze et al.

Title Page

Abstract

Introduction

Conclusions

References

Tables

Figures



Back

Close

Full Screen / Esc

Printer-friendly Version

Interactive Discussion



Nutrients and oxygen budgets in the North-East Atlantic

G. Maze et al.

Title Page

Abstract

Introduction

Conclusions

References

Tables

Figures



Back

Close

Full Screen / Esc

Printer-friendly Version

Interactive Discussion

which can be inferred from oxygen and nutrients fluxes and budget (Álvarez et al., 2003). On the other hand air-sea oxygen fluxes are necessary to differentiate the ocean and land sinks of the atmospheric anthropic carbon (Bopp et al., 2002). This study is thus an attempt to provide estimates of nutrients and oxygen fluxes constrained by observations.

Over the past decade, every two years from 2002 to 2010, the OVIDE project (<http://www.ifremer.fr/lpo/ovide/>) performed a Greenland to Portugal high resolution hydrographic survey (about 40 km between each stations). All cruises sampled high quality measurements of standard tracers such as temperature, salinity, nitrate, phosphate and oxygen. Each R/V *rosette* were equipped with an Acoustic Doppler Current Profiler (ADCP) and each survey thus provides a velocity field estimate from the surface to the bottom. These data were combined with thermal wind velocity estimates from hydrography and with Ekman current estimates from satellite data and optimized in a least square sense by Lherminier et al. (2007, 2010) and Gourcuff et al. (2011) to obtain an accurate absolute velocity field normal to the cruise track. From there, tracer transports and their associated errors can be estimated. The interannual OVIDE dataset is an unique opportunity to compute a decade long climatology of accurate tracer transports.

In this study we thus propose to use all available tracer transports to date through the OVIDE path – i.e. 2002, 2004 and 2006 – (2008 and 2010 velocity fields are still ongoing analysis) to compute their decadal climatology. Essentially, we propose to combine these transports with transport estimates through the Greenland-Scotland Ridge – quantities well documented from observations in the bibliography – to compute mass, nutrients and oxygen budgets for the North-East Atlantic, defined here as the area between the OVIDE path and the Greenland-Scotland Ridge (see Fig. 1).

The paper is organized as follow. In Sect. 2 we describe the domain and the tracer conservation model. In Sect. 3 we analyze the mass, nutrients and oxygen budgets. Air-sea oxygen fluxes are decomposed in details in Sect. 4. Results are discussed in Sect. 5 and we conclude in Sect. 6.

2 Domain and model

In this section we describe the domain of analysis and the model used to constraint the circulation, biological source/sink terms and air-sea oxygen fluxes for the North-East Atlantic Ocean.

2.1 Domain

The domain of analysis is shown in Fig. 1a, for which a schematic view is given in the same figure, panel b. The domain is bounded by the OVIDE survey track (red marks) on the south-western flank and by the Greenland-Scotland ridge (GSR, blue marks) on the north-eastern flank. We split the domain along the Reykjanes Ridge (RR, black marks) into two boxes: one to the north referred to as the “Irminger” box and one to the south referred to as the “North Eastern European Basin” (NEEB) box. Both boxes extend vertically from the air-sea interface to the bottom topography. Here after in the study variables related to: (i) the Irminger and NEEB boxes are labeled using subscripts “*n*” and “*s*” (ii) the vertical westernmost and easternmost faces are labeled using “*w*” and “*e*” (iii) the vertical RR face using “*rr*” and (iv) the horizontal air-sea interface labeled using “*a*”. Fig. 1b provides an example of this convention to the face area *A*.

Tracer properties on box faces were required. On westernmost faces we used the interannual mean of OVIDE data for 2002, 2004 and 2006 (Lherminier et al., 2007, 2010; Gourcuff et al., 2011). For all the other faces we used data from the World Ocean Atlas 2009 (Garcia et al., 2005, WOA09). The WOA09 grid is also used to provide complementary box properties such as horizontal and vertical surfaces or volume. Note that a similar horizontal domain was used by Lherminier et al. (2010) to constraint the volume flux across the Reykjanes Ridge. Here we extend their analysis to nutrients and oxygen fluxes.

BGD

9, 4323–4360, 2012

Nutrients and oxygen budgets in the North-East Atlantic

G. Maze et al.

Title Page

Abstract

Introduction

Conclusions

References

Tables

Figures

◀

▶

◀

▶

Back

Close

Full Screen / Esc

Printer-friendly Version

Interactive Discussion

2.2 Model

The model is a linear set of constraints constituted of mass, nutrients (nitrate N, phosphate P), oxygen solubility (O^s) and total oxygen (O) conservation equations for the Irminger and NEEB boxes as well as their junction.

It would be possible to estimate a set of parameters to compute separately each of these constraints. However, on one hand these estimates could eventually be inconsistent with each others and on the other hand some of the terms (biological and air-sea fluxes), poorly known, would be de facto determined as residuals to close the budgets. Here, we are interested in using a method to reconcile these parameters and their a priori estimates so that all conservation equations, or budgets, are being satisfied simultaneously. Such a classic optimization problem is tackled here using a linear inversion procedure described in Appendix A. This method increases the physical and biogeochemical consistency of the system and thus improve our knowledge of thereof.

For each of these 3 domains, we write the following sub-set of equations:

$$0 = \nabla T \quad (1)$$

$$0 = \nabla N T + B \quad (2)$$

$$0 = \nabla P T + r_{P:N} B \quad (3)$$

$$0 = \nabla O^s T + J^a \quad (4)$$

$$0 = \nabla O T + B' + J^a \quad (5)$$

where ∇ stands for the horizontal divergence operator (see Appendix B for more details). The first r.h.s. terms are thus the mass and tracer transport divergence: T are mass transports and N , P , O^s , O are tracer concentrations on box faces. Note that horizontal tracer transports are non-linear terms if one assume that both tracer concentrations and velocities have to be optimized. In order to keep the model as simple as possible, we hypothesized that only velocities require optimization. In other word, we assumed that between tracer concentrations and circulation, the former is the best

BGD

9, 4323–4360, 2012

Nutrients and oxygen budgets in the North-East Atlantic

G. Maze et al.

Title Page

Abstract

Introduction

Conclusions

References

Tables

Figures

◀

▶

◀

▶

Back

Close

Full Screen / Esc

Printer-friendly Version

Interactive Discussion

known. Doing so, tracer transports terms are linear with regard to the optimization procedure.

B is the net top to bottom biological vertical flux for nutrients in Eqs. (2)–(3). Thus B is the integrated result of the organic matter production (nutrients sink) and remineralization (nutrients source). A negative B then relates to organic matter production. We assumed that respiration/photosynthesis and remineralisation of organic matter happen at constant stoichiometric ratio for nitrate and phosphate: $r_{P:N} = 1/16$ (Anderson, 1995). Nitrate conservation equation does not make explicit mentions of atmospheric deposition in open ocean and coastal waters, river runoff supply and denitrification effects. Álvarez et al. (2002) provide an estimate of each of these terms north of the WOCE A25 4× cruise which is close to the OVIDE survey. It appears that denitrification almost balances the other two processes. The residual falls in the error estimate of the nitrate conservation equation used here.

J^a is the air-sea abiotic oxygen flux in Eqs. (4)–(5). A positive J^a is a source of oxygen, i.e. a downward flux leading to an oceanic oxygen uptake. J^a is examined in details in Sect. 4.

Last, B' is the net top-to-bottom biological source/sink term of oxygen (Eq. 5). For the optimization procedure to be efficient, it is necessary to relate B' to B , otherwise the nutrients conservation equations would be useless to improve our knowledge of the total oxygen budget terms. Broecker (1974) first introduced the concept of a conservative water mass tracer (which was then called “NO”) based on fixed stoichiometric relations of non-conservative tracers. It is based on the idea that the increase in preformed nitrate due to nitrate introduction during respiration balances the oxygen consumption. This leads to the conservation equation of preformed nitrate being a conservative tracer formulation. Preformed nitrate is given by (Pérez et al., 2005):

$$N^p = N - AOU/r_{O:N} \quad (6)$$

BGD

9, 4323–4360, 2012

Nutrients and oxygen budgets in the North-East Atlantic

G. Maze et al.

Title Page

Abstract

Introduction

Conclusions

References

Tables

Figures

⏪

⏩

◀

▶

Back

Close

Full Screen / Esc

Printer-friendly Version

Interactive Discussion



with $r_{O:N} = 150/16$. Taking the difference of Eq. (4) with Eq. (5) gives the AOU conservation equation:

$$0 = \nabla AOUT - B' \quad (7)$$

We take the AOU out of Eq. (6) and use Eq. (2) to obtain:

$$\begin{aligned} 0 &= -r_{O:N} \nabla N^p T + r_{O:N} \nabla N T - B' \\ 0 &= \nabla N^p T + B + B' / r_{O:N} \end{aligned} \quad (8)$$

Assuming that preformed nitrate is indeed a conservative tracer, we obtain $B' = -r_{O:N} B$ which allows us to link the total oxygen conservation Eq. (5) to those for nutrients N and P. We are aware that this also assumes the fact that dissolved organic matter remineralisation happens with a similar stoichiometric ratio as $r_{O:N}$. This assumption will be discussed in the next section.

Mass, nitrate, phosphate, oxygen solubility and total oxygen conservation equations for the Irminger and NEEB boxes as well as the whole domain thus provide a set of 15 linear constraints. To determine the a priori state of parameters, we used for the western most faces of boxes the 2002–2004–2006 mean of OVIDE mass and tracer transports. For all the other faces we used tracer data from the World Ocean Atlas 2009 (Garcia et al., 2005) and standard bibliographical transport estimates. The detailed description of the a priori state used to inverse this set of constraints is given in Appendix C. Parameters are listed together with their a priori estimates and errors in Table 1.

Each constraints residual error bar is set to $0.05 \times 10^9 \text{ kg s}^{-1}$ for mass, 10 kmol s^{-1} for nitrate, 2 kmol s^{-1} for phosphate and 100 kmol s^{-1} for oxygen solubility and total oxygen. This aims to represent a compromise between the a priori constraints residuals and upper bounds of the uncertainties of the tracer conservation equations due to interdecadal variability (i.e. the amplitude of the tracer time derivative omitted in conservation equations).

Nutrients and oxygen budgets in the North-East Atlantic

G. Maze et al.

Title Page

Abstract

Introduction

Conclusions

References

Tables

Figures



Back

Close

Full Screen / Esc

Printer-friendly Version

Interactive Discussion



3 Mass, nutrients and oxygen budgets

In this section we present results for the linear optimization of mass, nutrients and oxygen budgets.

3.1 Mass budget

Optimized mass transports are given in Table 2. The mass is conserved for each box as well as the whole domain and it has been verified that transport estimates are consistent with those from Lherminier et al. (2010).

Top to bottom mass transports induce a flow across the OVIDE track of $14.1 \pm 0.8 \times 10^9 \text{ kg s}^{-1}$ into the NEEB box. $9.3 \pm 0.7 \times 10^9 \text{ kg s}^{-1}$ of this transport is carried to the Irminger box through the RR while $4.8 \pm 0.5 \times 10^9 \text{ kg s}^{-1}$ are exported toward the Nordic Seas through the Iceland-Scotland Ridge. In the Irminger box, the RR northward transport combines with an additional influx across the Denmark Strait of $4.3 \pm 0.4 \times 10^9 \text{ kg s}^{-1}$ to balance a southwestward export through the OVIDE track of $13.7 \pm 0.8 \times 10^9 \text{ kg s}^{-1}$.

Thus if one account for the OVIDE face as 100 % of the NEEB (Irminger) box mass import (export), 30 % of these are taken to (out of) the Nordic Seas while 70 % are redistributed between both boxes through the RR.

3.2 Nutrients budget

Each of the constraints terms determined using the optimized parameters are given in Fig. 2a and b for nitrate and phosphate. All constraints on nutrients conservations are satisfied within the imposed error estimates.

Like mass transports, it is found that about 70 % of the nitrate import from the OVIDE section is taken to the Irminger Sea through the RR while 30 % are exported to the Nordic Seas. A residual convergence is found but with a large error estimate. The optimisation method we used thus shows here its interest. With a simple residual estimate

BGD

9, 4323–4360, 2012

Nutrients and oxygen budgets in the North-East Atlantic

G. Maze et al.

Title Page

Abstract

Introduction

Conclusions

References

Tables

Figures

◀

▶

◀

▶

Back

Close

Full Screen / Esc

Printer-friendly Version

Interactive Discussion



we would not be able to call on the biological term amplitude. But our inverse model procedure does combine information from nitrate, phosphate and oxygen simultaneously to optimize the B term. This explains why for the nitrate budget B is found to be about twice as large as the transports divergence it is supposed to balance (which also leads to constraints residual being different than zero, although budgets are closed within the constraint errors range).

Thus for the NEEB box, a nitrate transports convergence is balanced by a biological negative (sink) term of amplitude $B_s = -8.4 \pm 6.6 \text{ kmol s}^{-1}$. For the Irminger box, nitrate transports also converge and the biological term has an amplitude relatively similar to the NEEB box of $B_n = -7.8 \pm 6.5 \text{ kmol s}^{-1}$. Thus for the entire domain the net biological term is significantly negative and of amplitude $-16.2 \pm 9.3 \text{ kmol s}^{-1}$. Note that phosphate figures are mostly consistent with nitrate's using the constant ratio $r_{P:N}$.

The distribution of the biological terms in the two boxes thus points to the region between the OVIDE track and the Greenland-Scotland Ridge as a net producer of organic matter.

3.3 Oxygen solubility and total oxygen budgets

The oxygen solubility and total oxygen budget terms determined using optimized parameters are given in Fig. 3a and b. The oxygen solubility transport terms are driven by heat transports. Therefore it is not surprising to find a net oxygen solubility export through the OVIDE section ($-593 \pm 352 \text{ kmol s}^{-1}$, southward) because of the net heat import into the domain (Lherminier et al., 2010). Horizontal oxygen solubility transports diverge over both boxes which leads to an oceanic abiotic oxygen in-gassing of $264 \pm 66 \text{ kmol s}^{-1}$ and $444 \pm 70 \text{ kmol s}^{-1}$ over the Irminger and NEEB boxes respectively. We will show in the next Sect. 4 that this in-gassing is driven by air-sea heat flux cooling, although vertical mixing does play a none negligible role over the NEEB box.

Total oxygen transports across the OVIDE section also show a significant export ($-924 \pm 314 \text{ kmol s}^{-1}$, southward). This is due to the fact that subtropical oxygen-poor waters are transported northward (in the NEEB box) while subpolar oxygen-rich

Nutrients and oxygen budgets in the North-East Atlantic

G. Maze et al.

Title Page

Abstract

Introduction

Conclusions

References

Tables

Figures

⏪

⏩

◀

▶

Back

Close

Full Screen / Esc

Printer-friendly Version

Interactive Discussion



waters are transported southward (out of the Irminger box). Unlike nutrients, oxygen does show a significant southward export. Horizontal transports diverge over both boxes. This divergence is balanced by an abiotic air-sea in-gassing and a net biological source term due to the photosynthesis by the organic matter produced in the area (see nutrients budgets). The oceanic oxygen uptake by abiotic air-sea fluxes are $264 \pm 66 \text{ kmol s}^{-1}$ and $443 \pm 70 \text{ kmol s}^{-1}$ over the Irminger and NEEB boxes while the biological oxygen production rates are $73 \pm 61 \text{ kmol s}^{-1}$ and $79 \pm 62 \text{ kmol s}^{-1}$. The biological source term of oxygen thus points to the region between the OVIDE track and the Greenland-Scotland Ridge as an autotrophic region. We conducted a sensitivity study of the biological oxygen term to the Redfield ratio used to relate nitrate to oxygen biological fluxes. Although the model does show a sensitivity to the $r_{\text{O:N}}$ ratio (not shown) it is largely smaller than error bars and thus cannot be isolated significantly.

4 Air-sea oxygen flux partitioning

When surface mixed layer water masses are under or over saturated in oxygen, an air-sea oxygen flux is necessary to maintain a continuous oxygen partial pressure at the air-sea interface. Under/over saturation can be due to physical and biological processes modifying the oxygen concentration of the surface layers. Therefore, the total air-sea oxygen flux can be partitioned into abiotic and biotic contributions.

The abiotic air-sea oxygen flux component is often computed using air-sea heat fluxes and is referred to as the thermal component (Keeling et al., 1993). However, all diabatic processes, such as air-sea heat fluxes, but also water mass mixing can change water mass temperature and thus solubility to possibly trigger abiotic oxygen air-sea fluxes. It is thus of primary interest to determine the relative contribution of air-sea heat fluxes versus mixing processes to the abiotic air-sea oxygen flux in order to test the validity of the classic method using air-sea heat fluxes only.

BGD

9, 4323–4360, 2012

Nutrients and oxygen budgets in the North-East Atlantic

G. Maze et al.

Title Page

Abstract

Introduction

Conclusions

References

Tables

Figures

⏪

⏩

◀

▶

Back

Close

Full Screen / Esc

Printer-friendly Version

Interactive Discussion

The total abiotic air-sea oxygen flux is decomposed into a thermal (θ superscript) and a mixing (H superscript) component:

$$J^a = J^{a,\theta} + J^{a,H} \quad (9)$$

Following Keeling et al. (1993) the air-sea thermal oxygen flux can be determined as:

$$J^{a,\theta} = -\frac{\partial O_2^{\text{sol}}}{\partial \theta} \frac{Q_{\text{net}}}{c_p} \quad (10)$$

where O_2^{sol} is the oxygen solubility (Benson and Krause Jr., 1984), c_p the sea water specific heat (Millard and Fofonoff, 1983) and Q_{net} the air-sea heat flux (positive upward, cooling the ocean). Using WOA09 surface averaged temperature and oxygen we also determined the annual mean oxygen solubility dependence on temperature to be $-6.9 \mu\text{mol kg}^{-1} \text{ } ^\circ\text{C}^{-1}$ and $-5.4 \mu\text{mol kg}^{-1} \text{ } ^\circ\text{C}^{-1}$ in the Irminger and NEEB boxes.

Several methods can be used to determine the air-sea heat flux to be used in Eq. (10). The most direct one would be to use a gridded air-sea heat flux product and to compute a surface average for the two boxes. However, there are no such product with a sufficient resolution to properly resolve the East-Greenland Current and the large oceanic heat loss taking place in this western boundary current. The method we choose is in line with our study. Indeed, using optimized mass transports and temperatures from OVIDE and WOA09 data, we can compute horizontal heat transports for each of the model box faces and then define air-sea heat fluxes as their divergence. This method has the advantage (i) to be coherent with our oxygen solubility flux estimates and (ii) to take into account the heat transport by the EGC (because it is resolved by OVIDE transport estimates). We obtained horizontal heat transports in line with bibliographic standards (not shown) and we found that $221 \pm 30 \text{ W m}^{-2}$ and $72 \pm 13 \text{ W m}^{-2}$ of heat were removed from the Irminger and NEEB boxes at the surface in order to balance the heat budgets (error bars on those fluxes are from heat transport errors propagation in the divergence operator).

Nutrients and oxygen budgets in the North-East Atlantic

G. Maze et al.

Title Page

Abstract

Introduction

Conclusions

References

Tables

Figures

⏪

⏩

◀

▶

Back

Close

Full Screen / Esc

Printer-friendly Version

Interactive Discussion



Using these surface heat flux estimates into Eq. (10) finally lead to abiotic thermal in-gassing flux estimates $J^{a,\theta}$ of: $239 \pm 65 \text{ kmol s}^{-1}$ and $287 \pm 102 \text{ kmol s}^{-1}$ for the Irminger and NEEB boxes respectively.

The mixing component $J^{a,H}$ is driven by the mixed layer dynamic and the induced mixing of water masses with different temperature/salinity and oxygen properties. The non-linear relationship between temperature (and to a lesser degree salinity) and solubility can result in the saturation of a mixed water parcel to be different than the arithmetic mean saturation of its original components which can trigger in/out gassing (see Dietze and Oschlies, 2005, for instance). Here, we determined $J^{a,H}$ by taking the difference of the abiotic thermal flux with the total abiotic one. We obtained an oceanic oxygen uptake by $J^{a,H}$ of $25 \pm 92 \text{ kmol s}^{-1}$ and $156 \pm 123 \text{ kmol s}^{-1}$ for the Irminger and NEEB boxes respectively.

Last, estimating the biotic air-sea oxygen flux in our model is straightforward. Indeed, in the total oxygen budget, what is not horizontal transport and abiotic must be balanced by a biotic air-sea flux. In other word, the top to bottom biological term can only be balanced by a biotic air-sea flux. This leads to a biotic oxygen out-gassing of $-73 \pm 61 \text{ kmol s}^{-1}$ and $-79 \pm 62 \text{ kmol s}^{-1}$ for the Irminger and NEEB boxes.

All air-sea oxygen fluxes components derived here-above are summarized in Fig. 4. We obtained a total air-sea oxygen in-gassing flux of $191 \pm 90 \text{ kmol s}^{-1}$ and $365 \pm 93 \text{ kmol s}^{-1}$ for the Irminger and NEEB boxes. Only the biotic flux component out-gasses oxygen to the atmosphere. We note that its absolute amplitude is about 20% the abiotic one. Over the Irminger box the abiotic air-sea oxygen flux is driven by the thermal component, presumably because of the large heat flux cooling along the EGC. Over the NEEB box, the mixing in-gassing component is about half the thermal one. This shows that mixing induced air-sea oxygen fluxes can contribute significantly to the overall oceanic oxygen uptake in the region.

Nutrients and oxygen budgets in the North-East Atlantic

G. Maze et al.

Title Page

Abstract

Introduction

Conclusions

References

Tables

Figures

⏪

⏩

◀

▶

Back

Close

Full Screen / Esc

Printer-friendly Version

Interactive Discussion



5 Discussion

5.1 Mass

The mass budget provides mass transport estimates through all the faces of the boxes. We note that if one account for OVIDE faces as 100 % of each box import/export, 30 % of these are taken to/out of the Nordic Seas while 70 % are redistributed between both boxes through RR. This simple distribution emphasizes the crucial role played by the circulation through the Reykjanes Ridge region to link the Iceland Basin to the Irminger Sea. This mass transport is the less a priori constrained and is therefore the most affected by the optimization method. That is why more observational studies are necessary for a better estimate of this circulation.

5.2 Nutrients

Because phosphate fluxes are proportional to nitrate fluxes through a constant Redfield ratio, we only discuss nitrate in the following. Nutrients transports and fluxes are thus implicitly for mol of nitrate.

We determined an optimized estimate – relevant for the decadal timescale – for the net nitrate transport through the westernmost face of the domain of $11 \pm 16 \text{ kmol s}^{-1}$: i.e. no significant import through the OVIDE transect. We note that this figure derives from the a priori one ($12 \pm 31 \text{ kmol s}^{-1}$) which in turn, is the average of the 2002, 2004 and 2006 OVIDE surveys. Nitrate transports for those years are: $-1 \pm 49 \text{ kmol s}^{-1}$, $16 \pm 37 \text{ kmol s}^{-1}$ and $20 \pm 32 \text{ kmol s}^{-1}$. One could wonder how individual OVIDE nitrate transports figures compare with other studies? We indicated in the introduction of this study that Álvarez et al. (2002) derived a nitrate budget for a subpolar box north of the WOCE A25 4× 1997 survey but that their transport estimates have been improved by Lherminier et al. (2007) using additional constraints based on ADCP data, so that their nitrate transport and budget have to be updated. Using these new transport estimates (Lherminier et al., 2007) we computed the nitrate transport across the WOCE A25

BGD

9, 4323–4360, 2012

Nutrients and oxygen budgets in the North-East Atlantic

G. Maze et al.

Title Page

Abstract

Introduction

Conclusions

References

Tables

Figures

⏪

⏩

◀

▶

Back

Close

Full Screen / Esc

Printer-friendly Version

Interactive Discussion

4× survey and obtained a southwestward export of $-16 \pm 36 \text{ kmol s}^{-1}$, a significant reduction from the original value of $-50 \pm 19 \text{ kmol s}^{-1}$. This updated transport is not in line with individual OVIDE estimates regarding the sign, however uncertainties still make them compatible.

All these individual nitrate transports reveal that no significant transport on the decadal time scale can hide a large interannual variability. One must note however, that error bars make also possible a null net transport for each of those years. Our choice of combining OVIDE data with a climatological dataset – imposed by a lack of observations – thus cannot be ruled out. Whether no net transport is a consequence of insufficient interannual sampling or is effectively a characteristic of the decadal time scale remains to be determined. Including transports from the 2008 and 2010 OVIDE surveys (not yet available at the time of this study) as well as improving error bars in transport estimates will be necessary to conclude with further confidence.

Primarily because the top to bottom western NEEB box face is richer in nitrate than the other two faces, the nitrate optimized transports lead to a horizontal convergence in the NEEB box. If, as hypothesized, no nitrate accumulation is taking place in the NEEB box, this convergence has to be balanced by a biological sink term ($-8.4 \pm 6.6 \text{ kmol s}^{-1}$ which corresponds to about 4 % of the western face transport). This indicates that the NEEB box is an area of nutrients biological consumption or organic matter production. Lherminier et al. (2010) determined – using the upper bound of the deep waters potential density surface as a vertical limit between a surface and a deep box – that the NEEB box is primarily an upwelling region. This brings upward the deeper thermocline waters and Antarctic Bottom Water (AABW) which are rich in nutrients (McCartney et al., 1991). This large scale entrainment of deep nutrient rich water masses toward the surface layers thus suggests that the organic matter consuming nutrients in the NEEB box may be produced locally instead of being advected from the subtropical gyre water masses.

The Denmark Strait overflow and the East Greenland Current together carry $55 \pm 5 \text{ kmol s}^{-1}$ of NO_3 into the Irminger box while $192 \pm 11 \text{ kmol s}^{-1}$ are exported southward

Nutrients and oxygen budgets in the North-East Atlantic

G. Maze et al.

Title Page

Abstract

Introduction

Conclusions

References

Tables

Figures

⏪

⏩

◀

▶

Back

Close

Full Screen / Esc

Printer-friendly Version

Interactive Discussion

through the OVIDE section face. This would create a nitrate divergence in the Irminger Sea if no nitrate would have been carried in through the RR ridge. Indeed, this large flux of nitrate is able to turn the divergence into a convergence, which leads to a net biological consumption of nitrate ($-7.8 \pm 6.5 \text{ kmol s}^{-1}$) to close the budget. Like the NEEB box, the Irminger Sea is an area of organic matter production. As pointed out by Lherminier et al. (2010), the Irminger Sea is primarily a downwelling region. Thus nutrients required for organic matter production cannot mainly originate from the local deep layers. Instead, it is likely that a large fraction of those nutrients are imported from the NEEB box through the RR.

Álvarez et al. (2002) found the area north of the 1997 WOCE A25 4× section to be a net producer of nitrate from organic matter consumption. Using our updated nitrate transport across this section and their other nitrate input/output term estimates, the net production of nitrate north of the WOCE A25 4× section becomes 6.6 kmol s^{-1} , a large decrease since their original estimate of 40.6 kmol s^{-1} . However, this biological nitrate production is still of the opposite sign of our estimate. One should note that their budget was derived for the entire region north of the WOCE A25 4× section. Our results for the region between the OVIDE transect and the Greenland-Scotland Ridge, thus indicate that if there is a net biological production of nitrate north of the WOCE A25 4× section, it is probably confined to the Nordic Seas.

5.3 Oxygen

In our model, biological source/sink terms of oxygen are directly linked to those of nutrients. Therefore, the nitrate/phosphate biological consumption by organic matter production implies a net biological production of oxygen in the two boxes through photosynthesis. Our results thus point to the region between the OVIDE track and the Greenland-Scotland Ridge as being autotrophic, with a net production of oxygen at a rate of $73 \pm 61 \text{ kmol s}^{-1}$ and $79 \pm 62 \text{ kmol s}^{-1}$ over the Irminger and NEEB boxes respectively. A sensitivity test to the Redfield ratio $r_{\text{O:N}}$ has been conducted (not shown) but the sensitivity amplitude is indistinguishable from model error estimates. Thus, whether

BGD

9, 4323–4360, 2012

Nutrients and oxygen budgets in the North-East Atlantic

G. Maze et al.

Title Page

Abstract

Introduction

Conclusions

References

Tables

Figures

⏪

⏩

◀

▶

Back

Close

Full Screen / Esc

Printer-friendly Version

Interactive Discussion



the autotrophy amplitude in the region is significantly altered by the dissolved organic matter cycling or not cannot be significantly determined at this point.

Peng et al. (1987) analyzed a two years mooring timeserie between March 1983 and May 1985 located at 64° N, 27° W, i.e. in the Irminger Sea. They found a seasonal cycle of oxygen biological production rate with values from 0.3 in December to 12 mol m⁻² yr⁻¹ in May and an annual mean of 5.1 mol m⁻² yr⁻¹. If one attempt to extent this figure to the entire Irminger Sea, a scaling by the horizontal box surface leads to an oxygen production rate of 100 kmol s⁻¹. Our estimate of oxygen biological production is net, i.e. it also encouncts for respiration and remineralisation. Therefore it is re-ensuring to find a smaller figure than the one of Peng et al. (1987).

For a better understanding of the oxygen budget in the region, we also estimated air-sea oxygen biotic and abiotic fluxes and partitionned the latter between a thermal and a mixing component. Our total oxygen in-gassing estimates, scaled by the horizontal surface of each boxes, indicate that 9 ± 4 mol m⁻² yr⁻¹ and 4 ± 1 mol m⁻² yr⁻¹ of oxygen are fluxed into the ocean over the Irminger and NEEB boxes. These figures are relatively larger than bibliographical standards. For instance Najjar and Keeling (2000) found an in-gassing of about 2 mol m⁻² yr⁻¹ for the Atlantic ocean (see their Fig. 6) and Gruber et al. (2001) found a flux of about 0.5 mol m⁻² yr⁻¹ for the North Atlantic north of 53° N (see their Fig. 5). However, more localized and recent studies indicate that air-sea oxygen in-gassing flux can be large in the subpolar gyre. For instance, using mooring data Körtzinger et al. (2008) found a flux of 10 ± 3 mol m⁻² yr⁻¹ for the Labrador Sea. Our estimate for the Irminger Sea (9 ± 4 mol m⁻² yr⁻¹) is remarkably close to this direct observational value. The Irminger box is rather small compared to those used in previous budget estimates based on sparse trans-oceanic hydrographic surveys, this is probably why we obtained an oxygen flux in line with the local Körtzinger et al. (2008) estimate.

The abiotic air-sea oxygen flux partitionning into a thermal (due to air-sea heat flux) and a mixing component (due to water mass mixing) suggests that over the Irminger Sea the thermal component drives the air-sea flux. Dietze and Oschlies (2005) have

BGD

9, 4323–4360, 2012

Nutrients and oxygen budgets in the North-East Atlantic

G. Maze et al.

Title Page

Abstract

Introduction

Conclusions

References

Tables

Figures

⏪

⏩

◀

▶

Back

Close

Full Screen / Esc

Printer-friendly Version

Interactive Discussion

Nutrients and budgets in the North-East Atlantic

G. Maze et al.

Title Page

Abstract

Introduction

Conclusions

References

Tables

Figures



Back

Close

Full Screen / Esc

Printer-friendly Version

Interactive Discussion



shown in an eddy permitting model simulation of the North-Atlantic that the annual mean abiotic oxygen flux is overestimated by the thermal flux component at high latitudes because of a mixing induced out-gassing. Our results indicate that mixing induces in-gassing at high latitudes (Irminger box). However the error bar is large and the sign of this flux component is not significant in our model. On the other hand, over the NEEB box the abiotic mixing flux is significantly in-gassing the ocean with oxygen. The mixing flux takes an important role in the NEEB box because of the vertical oceanic oxygen structure. In this area, there is a strong oxygen minimum around the thermocline depth which is associated with water masses originating from the subtropical gyre and advected into the box through the southwestern face by the NAC (Van Aken et al., 1995, 1996; Sarafanov et al., 2008). Convective vertical mixing events erode and dilute these poorly saturated water masses to the surface which result in a large mixing flux in-gassing. We believe this mechanism to be robust. A poor representation of the seasonal mixed layer depth and thermocline structure in the Iceland Basin, as well as the restoring to 100 % of saturation on water mass they applied on open boundaries could explain why the Dietze and Oschlies (2005) study did not found similar conclusions. It is clear though, that further analysis are required to identify the role of mixing in air-sea oxygen fluxes.

5.4 Community production estimate

To finish this discussion, it is tempting to come back to the nutrients budget and to estimate a rate of community production of carbon. Because our budget encompasses surface and deeper processes, we are able to estimate a net community production (NCP). NCP takes place when primary production is greater than community respiration. It is an important measure of the strength of the biological pump and thus a process that must be considered in evaluating the marine cycling of carbon.

NCP, as nitrate-based carbon assimilation, can be estimated from biological source/sink terms of nitrate. Using state of the art constant stoichiometric ratios to describe the respiration/photosynthesis reactions of the marine organic matter (C:N:P:O₂

of 106:16:1:–150, see Anderson, 1995) we obtain for the Irminger and NEEB boxes NCP rates of $-51 \pm 43 \text{ kmolC s}^{-1}$ and $-56 \pm 44 \text{ kmolC s}^{-1}$. The biological net consumption of nitrate producing organic matter thus indicates that the region between the OVIDE track and the Greenland-Scotland Ridge is an area of carbon fixation. It is now well known that the Redfield ratio C:N of 6.6 used here may be an underestimate (see Sambrotto et al., 1993; Toggweiler, 1993, for instance). This also seems to be the case for the North East Atlantic open ocean (see Kahler and Koeve, 2001, discussion from the analysis of vertical profiles along the 20° W meridian between 33° N and 60° N in June/July 1996, relevant for our NEEB box). Then if more carbon is fixed per unit of nitrate taken up – a process usually referred to as carbon over-consumption – our NCP estimates are to be considered as lower bands of the actual values.

6 Conclusions

Using a state of the art optimization method and a linear model, we combined climatological data from the WOA09 with a 2002–2006 average estimate of transports from OVIDE surveys to conserve mass, nutrients, oxygen solubility and total oxygen over the North-East Atlantic Ocean.

The optimization method used here highlights that combining climatological data with hydrographic tracers and mass transport estimates – averaged over multiple years of survey – is feasible to obtain statistically significant estimates of non-conservative tracer budget residuals. However, a better sampling of the circulation of the North-East Atlantic is still required to lower error estimates. More precisely, we found that exchanges between the Irminger Sea and the Iceland Basin play a crucial role in the nutrients budgets, thus more observational estimates of the Reykjanes Ridge circulation region are required.

Our biological and air-sea oxygen flux estimates are realistic, suggesting that their analysis has some merit. We determined that the region between the OVIDE survey and the Greenland-Scotland Ridge is autotrophic and is a net organic matter production

BGD

9, 4323–4360, 2012

Nutrients and oxygen budgets in the North-East Atlantic

G. Maze et al.

Title Page

Abstract

Introduction

Conclusions

References

Tables

Figures

⏪

⏩

◀

▶

Back

Close

Full Screen / Esc

Printer-friendly Version

Interactive Discussion



Nutrients and oxygen budgets in the North-East Atlantic

G. Maze et al.

Title Page

Abstract

Introduction

Conclusions

References

Tables

Figures

⏪

⏩

◀

▶

Back

Close

Full Screen / Esc

Printer-friendly Version

Interactive Discussion

region. Our quantitative estimates of the Net Community Production of carbon could provide helpful indications to validate numerical simulations of the North-East Atlantic where both circulation and biological models still need improvements. Also our air-sea oxygen flux partitioning shows that (i) the thermal flux component alone can reasonably
5 represents the total flux in the Irminger Sea but that (ii) the still poorly studied abiotic mixing flux component can have a very significant impact on air-sea oxygen fluxes in the presence of a strong thermocline oxygen minimum. This latter results may have implications in determining the ocean and land sinks of the atmospheric anthropic carbon with methods based on net air-sea oxygen flux estimates from the thermal component
10 only.

Appendix A

Inverse method

Here we describe the inversion procedure used to optimize parameters of the model described in Sect. 2.2 and Appendix B. The procedure presented here is for a linear
15 model, the reader is referred to Tarantola and Valette (1982) and Mercier (1986) for further details on a non-linear formulation.

Let $\mathbf{X} = \{X^1, \dots, X^M\}$ refers to the finite set of M parameters needed to describe the system such as velocity, fluxes or tracer concentrations. A physical model will impose N constraints on the possible values of \mathbf{X} which can take the functional form:

$$f^1(X^1, \dots, X^M) = 0$$

$$f^2(X^1, \dots, X^M) = 0$$

...

$$f^N(X^1, \dots, X^M) = 0$$

Let \mathbf{X}_0 be an a priori state of information of the model parameters \mathbf{X} and \mathbf{E}_0 the associated error covariance matrix. We refer to the information after inversion as the a
25

posteriori or optimized state. The constraints take values $f(\mathbf{X})$ at \mathbf{X} and their error covariance matrix is denoted as \mathbf{E}_c . The optimization procedure minimizes the following function:

$$(\mathbf{X} - \mathbf{X}_0)^T \cdot \mathbf{E}_0^{-1} \cdot (\mathbf{X} - \mathbf{X}_0) + f(\mathbf{X})^T \cdot \mathbf{E}_c^{-1} \cdot f(\mathbf{X}) \quad (\text{A1})$$

5 where the superscript T indicates a transpose operator. The first term is the squared distance between the a priori and a posteriori estimates of the parameters while the second term is the constraints residual weighted by their errors.

The best estimate \mathbf{X}^* and its error covariance matrix \mathbf{E}^* are given uniquely by:

$$\mathbf{X}^* = \mathbf{X}_0 - \mathbf{Q} \cdot f(\mathbf{X}_0) \quad (\text{A2})$$

$$10 \quad \mathbf{E}^* = \mathbf{E}_0 - \mathbf{Q} \cdot \mathbf{F} \cdot \mathbf{E}_0 \quad (\text{A3})$$

where \mathbf{F} is the model matrix of partial derivatives (model jacobian)

$$\mathbf{F}^{ij} = \frac{\partial f^i}{\partial \mathbf{X}^j} \quad (\text{A4})$$

and the matrix \mathbf{Q} is given by:

$$\mathbf{Q} = \mathbf{E}_0 \cdot \mathbf{F}^T \cdot (\mathbf{F} \cdot \mathbf{E}_0 \cdot \mathbf{F}^T + \mathbf{E}_c)^{-1} \quad (\text{A5})$$

15 The set of constraints f^i used in this study are the equations Eqs. (1)–(5) written for each of the boxes and their junction (15 equations). The a priori state vector \mathbf{X}_0 and associated errors \mathbf{E}_0 are described in Appendix C and Table 1.

Appendix B

Model details

20 In Sect. 2.2 we presented a synthetic formulation of the model and conservation equations. Biological source/sink terms B and abiotic air-sea fluxes J^a are straightforward

Nutrients and nitrogen budgets in the North-East Atlantic

G. Maze et al.

Title Page

Abstract

Introduction

Conclusions

References

Tables

Figures

⏪

⏩

◀

▶

Back

Close

Full Screen / Esc

Printer-friendly Version

Interactive Discussion

terms that do not need more details. On the other hand, tracer transports divergence for a tracer C are given more precisely by:

$$\nabla C T = C_w T_w - C_e T_e + \alpha C_{rr} T_{rr} \quad (\text{B1})$$

where C is 1 for mass transports otherwise it is the mean tracer concentrations on box faces, T_i are mass transports across the box faces and the coefficient α is -1 for the NEEB box, 1 for the Irminger box and 0 for the entire domain. For the model to be linear, only mass transports are optimized by the inversion procedure.

The mass transport T_w is taken from OVIDE data while mass transports T_e, T_{rr} across the eastern and RR faces are computed as ρF using density ρ from the WOA09 data and volume fluxes F from the bibliography (see details in the next appendix).

Tracer concentrations are determined as follows:

- Along western faces, C_w are computed using tracer and mass transports from OVIDE data (see next appendix) as: $C_w = T_w^C / T_w$. For a top-to-bottom estimate, this is a much better approximation than the simple face average tracer concentration.
- Along eastern faces, C_e are computed as:

$$C_e = \frac{C_e^{\text{top}} \rho_e^{\text{top}} F_e^{\text{top}} + C_e^{\text{bottom}} \rho_e^{\text{bottom}} F_e^{\text{bottom}}}{\rho_e F_e} \quad (\text{B2})$$

where “top” and “bottom” upperscripts stand for the top (mainly going northward) and bottom (mainly going southward) layer properties. We adopted this simple method to better represent the strong vertical shear in tracer properties that could not be captured by the top to bottom average used in the model. F are volume fluxes taken from the bibliography while tracer concentrations C and density ρ are computed from the WOA09.

- Along the Reykjanes Ridge, we used face averaged concentrations from the WOA09.

BGD

9, 4323–4360, 2012

Nutrients and oxygen budgets in the North-East Atlantic

G. Maze et al.

Title Page

Abstract

Introduction

Conclusions

References

Tables

Figures

⏪

⏩

◀

▶

Back

Close

Full Screen / Esc

Printer-friendly Version

Interactive Discussion



These methods allow for a simple top-to-bottom linear conservation model formulation to make use of observational estimates while, at the same time, to take into account the water mass and circulation basic vertical structure.

Appendix C

5 A priori state of the model

– Transports across western box faces

Western box faces are defined along the OVIDE cruise track because we want to make use of the OVIDE survey data. Mass, nutrients, oxygen solubility and total oxygen transports across western box faces are given by:

$$10 \quad T_w^C = \int_{ip=1}^{n_p} \int_{iz=1}^{N_i} C(ip, iz) \rho_w(ip, iz) U_w(ip, iz) dS \quad (C1)$$

where ip is a station pair and iz a vertical level. C is 1 to compute mass transports, otherwise it is the tracer transported concentration. U_w are normal absolute velocities from a ship ADCP-constrained inverse model (see Lherminier et al., 2007, 2010; Gourcuff et al., 2011). We used OVIDE tracer and velocity data available for 2002, 2004 and 2006. The list of station pair indexes to integrate over for the southern and Irminger boxes thus depends on the OVIDE cruise year. Error estimates are obtained from the error covariance matrix $\mathbf{M}(N_p, N_p)$ of the Lherminier et al. (2010) inverse model following:

$$15 \quad er(T_w) = \iint \sqrt{(C\rho_w dS)^T \cdot \mathbf{M} \cdot (C\rho_w dS)} \quad (C2)$$

where upperscript T is the transpose matrix operator. We determined mass, nutrients and oxygen transports and their associated errors for the OVIDE survey of

BGD

9, 4323–4360, 2012

Nutrients and oxygen budgets in the North-East Atlantic

G. Maze et al.

Title Page

Abstract

Introduction

Conclusions

References

Tables

Figures

⏪

⏩

◀

▶

Back

Close

Full Screen / Esc

Printer-friendly Version

Interactive Discussion



Nutrients and oxygen budgets in the North-East Atlantic

G. Maze et al.

Title Page

Abstract

Introduction

Conclusions

References

Tables

Figures

⏪

⏩

◀

▶

Back

Close

Full Screen / Esc

Printer-friendly Version

Interactive Discussion



2002, 2004 and 2006, and then computed their time average. Because of the linear model formulation (tracer concentrations are not optimized, only mass transports are), we computed tracer concentrations along the OVIDE box faces as $C_w = T_w^C / T_w^\rho$ to keep making use of the a priori tracer transport estimates using Eq. (C1).

– Transports across the other box faces

As pointed out in Appendix B we used WOA09 mean tracer and density concentrations for top and bottom layers. Volume fluxes are from the bibliography:

– Denmark Strait

Flux $F_{ne} = -4.3 \pm 2.2$ Sv is the sum of the IIC = 0.7 ± 0.6 Sv (Icelandic Irminger Current, Jónsson and Valdimarsson, 2005), the EGC = -2 ± 1 Sv (East Greenland Current, Pickart et al., 2005) and the DSOW = -3 ± 1 Sv (Denmark Strait Overflow, Macrander et al., 2005; Dickson et al., 2008)

– Between the Southern and Northern boxes

Flux $F_{rr} = 12 \pm 5$ Sv is the volume flux over the Reykjanes Ridge estimated from the range of 9.3–15.6 Sv (Treguier et al., 2005; Bower et al., 2002).

– Between Iceland and Scotland

Flux $F_{se} = 4.7 \pm 2.2$ Sv is the sum of the ISI = 7.7 ± 2 Sv (Iceland-Shetland Inflow: 3.8 Sv in the Faroe branch and 3.9 Sv in the Shetland branch, Hansen et al., 2008) and ISOW = -3 ± 1 Sv (Iceland-Scotland Overflow: 1.9 ± 0.5 Sv at Faroe-Bank Channel and 1 ± 0.5 Sv across Iceland-Faroe, Hansen and Østerhus, 2007).

For the volume flux vertical decomposition in tracer transport estimates across the eastern faces we used:

- For the Irminger box, the top layer volume flux (-0.3 Sv) was considered to be the sum of the IIC (0.7 Sv) and half of the EGC (-1 Sv) while the bottom

layer volume flux (-4 Sv) is the sum of the DSOW (-3 Sv) and half of the EGC (-1 Sv). We considered the EGC to be barotropic.

- For the NEEB box, the top layer volume flux is the ISI (7.7 Sv) and the bottom one is the ISOW (-3 Sv).

– Air-sea oxygen abiotic fluxes

The abiotic flux can be partitioned into a thermal and a mixing component. Because there is no estimate of the later, we estimated the first one, double its value and associated a relative 200 % error. Following Keeling et al. (1993), the thermal flux component was computed using:

$$J^{\text{therm}} = -\frac{\partial O_2^{\text{sol}}}{\partial \theta} \frac{Q_{\text{net}}}{c_p} \quad (\text{C3})$$

where O_2^{sol} is the oxygen solubility (Benson and Krause Jr., 1984), c_p the sea water specific heat (Millard and Fofonoff, 1983) and Q_{net} the air-sea heat flux (positive upward cooling the ocean). We used the WOA09 monthly climatology of sea surface temperature and salinity to compute a monthly climatology of surface oxygen solubility and specific heat. We then used the third release of the Objectively Analyzed air-sea Fluxes data set (Yu et al., 2008, see <http://oafux.whoi.edu/>) to compute a monthly climatology of Q_{net} for the period 1998–2007. After surface integration over boxes and yearly averaging, we obtained a priori estimates of the thermal flux for the two boxes.

– Biological source/sink terms

The a priori estimate of B terms for the Irminger and NEEB boxes are based on observational NCP estimates from Lee (2001). They determined a regional net community production rates of 0.8 GtC yr^{-1} for the Atlantic Ocean between 40° N and 70° N . Using a surface of $12.4 \times 10^{12} \text{ m}^2$ and a C:N ratio of 106:16 this provides a B flux estimate of $0.81 \text{ mol yr}^{-1} \text{ m}^{-2}$ for nitrate. The a priori estimate of B terms

Nutrients and oxygen budgets in the North-East Atlantic

G. Maze et al.

Title Page

Abstract

Introduction

Conclusions

References

Tables

Figures

⏪

⏩

◀

▶

Back

Close

Full Screen / Esc

Printer-friendly Version

Interactive Discussion



for our model was then determined by scaling this flux with the horizontal surface of the Irminger and NEEB boxes and applying a 200 % relative error amplitude.

– Redfield ratios

Following Anderson (1995), the Redfield ratios are 16 for $r_{N:P}$ and $-150/16$ for $r_{O:N}$.

Acknowledgements. G. Maze was co-funded by the GIS Europole Mer, Ifremer and the CREST Argo project from the CPER Bretagne 2008–2013. The CREST Argo project is funded by Europe through the FEDER program and by the Brittany Region, Brest Metropole Océane and CG29. Funding for this work was also provided by the CARBOCHANGE FP7-ENV-2010 of the European Commission (264879) and by the Spanish Ministry of Education and Sciences through the CATARINA (CTM2010-17141/MAR). The OVIDE survey is a project co-funded by IFREMER, CNRS-INSU and LEFE. Contributions from H. Mercier and P. Morin was funded by the CNRS and from V. Thierry by the IFREMER.



The publication of this article is financed by CNRS-INSU.

References

- Álvarez, M., Bryden, H., Perez, F., Rios, A., and Roson, G.: Physical and biogeochemical fluxes and net budgets in the subpolar and temperate North Atlantic, *J. Mar. Res.*, 60, 191–226, 2002. 4325, 4329, 4336, 4338
- Álvarez, M., Ríos, A. F., Pérez, F. F., Bryden, H. L., and Rosón, G.: Transports and budgets of total inorganic carbon in the subpolar and temperate North Atlantic, *Global Biogeochem. Cy.*, 17, 1002–1023, doi:10.1029/2002GB001881, 2003. 4326

Nutrients and oxygen budgets in the North-East Atlantic

G. Maze et al.

Title Page

Abstract

Introduction

Conclusions

References

Tables

Figures



Back

Close

Full Screen / Esc

Printer-friendly Version

Interactive Discussion



Discussion Paper | Discussion Paper | Discussion Paper | Discussion Paper | Discussion Paper

- Anderson, L. A.: On the hydrogen and oxygen content of marine phytoplankton, *Deep Sea Res.* I, 42, 1675–1680, 1995. 4329, 4341, 4348
- Benson, B. and Krause Jr., D.: The concentration and isotopic fractionation of oxygen dissolved in freshwater and seawater in equilibrium with the atmosphere, *Limnol. Oceanogr.*, 29, 620–632, 1984. 4334, 4347
- 5 Bopp, L., Quéré, C. L., Heimann, M., Manning, A. C., and Monfray, P.: Climate-induced oceanic oxygen fluxes: Implications for the contemporary carbon budget, *Global Biogeochem. Cy.*, 16, 1022–1045, doi:10.1029/2001GB001445, 2002. 4326
- 10 Bower, A., Le Cann, B., Rossby, T., Zenk, W., Gould, J., Speer, K., Richardson, P., Prater, M., and Zhang, H.: Directly measured mid-depth circulation in the northeastern North Atlantic Ocean, *Nature*, 419, 603–607, 2002. 4346, 4355
- Brambilla, E. and Talley, L. D.: Subpolar Mode Water in the NorthEastern Atlantic. Part I: Averaged properties and mean circulation, *J. Geophys. Res.*, 113, C04025, doi:10.1029/2006JC004062, 2008. 4325
- 15 Brambilla, E., Talley, L. D., and Robbins, P. E.: Subpolar Mode Water in the NorthEastern Atlantic. Part II: Origin and transformation, *J. Geophys. Res.*, 113, C04026, doi:10.1029/2006JC004063, 2008. 4325
- Broecker, W. S.: NO, a conservative water-mass tracer, *Earth Planet. Sci. Lett.*, 23, 100–107, 1974. 4329
- 20 de Boisséson, E., Thierry, V., Mercier, H., Desbruyères, D., and Caniaux, G.: Origin, formation and variability of the Subpolar Mode Water located over the Reykjanes Ridge in the ORCA025-G70 simulation, submitted *J. Geophys. Res.*, in review, 2012. 4325
- de Boisséson, E., Thierry, V., Mercier, H., and Caniaux, G.: Mixed layer heat budget in the Iceland Basin from Argo, *J. Geophys. Res.*, 115, C10055, doi:10.1029/2010JC006283, 2010. 4325
- 25 Dickson, B. and Dye, S. and Jónsson, S. and K
”ohl, A. and Macrander, A. and Marnela, M. and Meincke, J. and Olsen, S. and Rudels, B. and Valdimarsson, H. and Voet, G.: The Overflow Flux West of Iceland: Variability, Origins and Forcing. In *Arctic–Subarctic Ocean Fluxes: Defining the Role of the Northern Seas in Climate.*, chap. 19, Springer Netherlands, 2008. 4346
- 30 Dietze, H. and Oschlies, A.: On the correlation between air-sea heat flux and abiotically induced oxygen gas exchange in a circulation model of the North Atlantic, *J. Geophys. Res.*, 110, C09016, doi:10.1029/2004JC002453, 2005. 4335, 4339, 4340

Nutrients and oxygen budgets in the North-East Atlantic

G. Maze et al.

[Title Page](#)[Abstract](#)[Introduction](#)[Conclusions](#)[References](#)[Tables](#)[Figures](#)[Back](#)[Close](#)[Full Screen / Esc](#)[Printer-friendly Version](#)[Interactive Discussion](#)

Nutrients and oxygen budgets in the North-East Atlantic

G. Maze et al.

Title Page

Abstract

Introduction

Conclusions

References

Tables

Figures

◀

▶

◀

▶

Back

Close

Full Screen / Esc

Printer-friendly Version

Interactive Discussion

- Eldevik, T., Nilsen, J. E. O., Iovino, D., Anders Olsson, K., Sando, A. B., and Drange, H.: Observed sources and variability of Nordic seas overflow, *Nature Geosci.*, 2, 406–410, 2009. 4325
- Falina, A., Sarafanov, A., and Sokov, A.: Variability and renewal of Labrador Sea Water in the Irminger Basin in 1991–2004, *J. Geophys. Res.*, 112, C01006, doi:10.1029/2005JC003348, 2007. 4325
- Garcia, H. E., Boyer, T. P., Levitus, S., Locarnini, R. A., and Antonov, J.: On the variability of dissolved oxygen and apparent oxygen utilization content for the upper world ocean: 1955 to 1998, *Geophys. Res. Lett.*, 32, L09604, doi:10.1029/2004GL022286, 2005. 4327, 4330
- Gourcuff, C., Lherminier, P., Mercier, H., and Le Traon, P. Y.: Altimetry combined with hydrography for ocean transport estimation, *J. Atmos. Ocean. Tech.*, 28, 1324–1337, doi:10.1175/2011JTECHO818.1, 2011. 4326, 4327, 4345
- Gruber, N., Gloor, M., Fan, S.-M., and Sarmiento, J. L.: Air-Sea Flux of Oxygen Estimated From Bulk Data: Implications For the Marine and Atmospheric Oxygen Cycles, *Global Biogeochem. Cy.*, 15, 783–803, doi:10.1029/2000GB001302, 2001. 4339
- Hansen, B. and Østerhus, S.: Faroe Bank Channel overflow 1995–2005, *Prog. Oceanogr.*, 75, 817–856, 2007. 4346
- Hansen, B., Østerhus, S., Turrell, W., Jónsson, S., Valdimarsson, H., Hátún, H., and Olsen, S.: The Inflow of Atlantic Water, Heat, and Salt to the Nordic Seas Across the Greenland-Scotland Ridge. In: *Arctic-Subarctic Ocean Fluxes: Defining the Role of the Northern Seas in Climate*, chap. 1, 15–43, Springer Netherlands, 2008. 4346
- Jónsson, S. and Valdimarsson, H.: The flow of Atlantic water to the North Icelandic Shelf and its relation to the drift of cod larvae, *ICES Journal of Marine Science: Journal du Conseil*, 62, 1350–1359, 2005. 4346
- Kahler, P. and Koeve, W.: Marine dissolved organic matter: can its C:N ratio explain carbon overconsumption?, *Deep Sea Res. I*, 48, 49–62, 2001. 4341
- Karstensen, J., Stramma, L., and Visbeck, M.: Oxygen minimum zones in the eastern tropical Atlantic and Pacific oceans, *Prog. Oceanogr.*, 77, 331–350, a New View of Water Masses After WOCE. A Special Edition for Professor Matthias Tomczak, 2008.
- Keeling, R. F., Najjar, R. P., Bender, M. L., and Tans, P. P.: What Atmospheric Oxygen Measurements Can Tell Us About the Global Carbon Cycle, *Global Biogeochem. Cy.*, 7, 37–67, doi:10.1029/92GB02733, 1993. 4333, 4334, 4347

Nutrients and oxygen budgets in the North-East Atlantic

G. Maze et al.

Title Page

Abstract

Introduction

Conclusions

References

Tables

Figures

⏪

⏩

◀

▶

Back

Close

Full Screen / Esc

Printer-friendly Version

Interactive Discussion



- Körtzinger, A., Send, U., Wallace, D. W. R., Karstensen, J., and DeGrandpre, M.: Seasonal cycle of O_2 and pCO_2 in the central Labrador Sea: Atmospheric, biological, and physical implications, *Global Biogeochem. Cy.*, 22, GB1014, doi:10.1029/2007GB003029, 2008. 4339
- 5 Kvaleberg, E., Haine, T. W. N., and Waugh, D. W.: Middepth spreading in the subpolar North Atlantic Ocean: Reconciling CFC-11 and float observations, *J. Geophys. Res.*, 113, C08019, doi:10.1029/2007JC004104, 2008. 4325
- Lee, K.: Global net community production estimated from the annual cycle of surface water total dissolved inorganic carbon, *Limnol. Oceanogr.*, 46, 1287–1297, 2001. 4347, 4355
- 10 Lherminier, P., Mercier, H., Gourcuff, C., Alvarez, M., Bacon, S., and Kermabon, C.: Transports across the 2002 Greenland-Portugal Ovide section and comparison with 1997, *J. Geophys. Res.*, 112, C07003, doi:10.1029/2006JC003716, 2007. 4325, 4326, 4327, 4336, 4345
- Lherminier, P., Mercier, H., Huck, T., Gourcuff, C., Perez, F. F., Morin, P., Sarafanov, A., and Falina, A.: The Atlantic Meridional Overturning Circulation and the subpolar gyre observed at the A25-OVIDE section in June 2002 and 2004, *Deep Sea Res. I*, 57, 1374–1391, 2010.
- 15 4326, 4327, 4331, 4332, 4337, 4338, 4345
- Macrander, A., Send, U., Valdimarsson, H., Jónsson, S., and Käse, R.: Interannual changes in the overflow from the Nordic Seas into the Atlantic Ocean through Denmark Strait, *Geophys. Res. Lett.*, 32, L06606, doi:10.1029/2004GL021463, 2005. 4346
- 20 McCartney, M. S., Bennett, S. L., and Woodgate-Jones, M. E.: Eastward Flow through the Mid-Atlantic Ridge at 11°N and Its Influence on the Abyss of the Eastern Basin, *J. Phys. Oceanogr.*, 21, 1089–1121, 1991. 4337
- Mercier, H.: Determining the General Circulation of the Ocean: A Nonlinear Inverse Problem, *J. Geophys. Res.*, 91, 5103–5109, 1986. 4342
- 25 Millard, R. J. and Fofonoff, P.: Algorithms for computation of fundamental properties of seawater, *Unesco technical papers in marine science*, UNESCO, 1983. 4334, 4347
- Najjar, R. G. and Keeling, R. F.: Mean Annual Cycle of the Air-Sea Oxygen Flux: A Global View, *Global Biogeochem. Cy.*, 14, 573–584, doi:10.1029/1999GB900086, 2000. 4339
- Peng, T. H., Takahashi, T., Broecker, W. S., and Olafsson, J.: Seasonal variability of carbon dioxide, nutrients and oxygen in the northern North Atlantic surface water: observations and a model, *Tellus B*, 39B, 439–458, 1987. 4339
- 30 Pérez, F. F., Castro, C. G., Rios, A. F., and Fraga, F.: Chemical properties of the deep winter mixed layer in the Northeast Atlantic (40–47° N), *J. Marine Syst.*, 54, 115–125, 2005. 4329

Nutrients and oxygen budgets in the North-East Atlantic

G. Maze et al.

Title Page

Abstract

Introduction

Conclusions

References

Tables

Figures

◀

▶

◀

▶

Back

Close

Full Screen / Esc

Printer-friendly Version

Interactive Discussion



- Pickart, R., Straneo, F., and Moore, G. W. K.: Is Labrador Sea Water formed in the Irminger basin?, *Deep-Sea Res. I*, 50, 23–52, 2003a. 4325
- Pickart, R., Spall, M. A., Ribergaard, M. H., Moore, G. W. K., and Milliff, R. F.: Deep convection in the Irminger Sea forced by the Greenland tip jet, *Nature*, 424, 152–156, 2003b. 4325
- 5 Pickart, R. S., Torres, D. J., and Fratantoni, P. S.: The East Greenland Spill Jet, *J. Phys. Oceanogr.*, 35, 1037–1053, 2005. 4346
- Sambrotto, R. N., Savidge, G., Robinson, C., Boyd, P., Takahashi, T., Karl, D. M., Langdon, C., Chipman, D., Marra, J., and Codispoti, L.: Elevated consumption of carbon relative to nitrogen in the surface ocean, *Nature*, 363, 248–250, 1993. 4341
- 10 Sarafanov, A., Falina, A., Sokov, A., and Demidov, A.: Intense warming and salinification of intermediate waters of southern origin in the eastern North Atlantic in the 1990s to mid-2000s, *J. Geophys. Res.*, 113, C12022, doi:10.1029/2008JC004975, 2008. 4340
- Schott, F. A., Zantopp, R., Stramma, L., Dengler, M., Fischer, J., and Wibaux, M.: Circulation and Deep-Water Export at the Western Exit of the Subpolar North Atlantic, *J. Phys. Oceanogr.*, 34, 817–843, 2004. 4325
- 15 Sproson, D. A. J., Renfrew, I. A., and Heywood, K. J.: Atmospheric conditions associated with oceanic convection in the south-east Labrador Sea, *Geophys. Res. Lett.*, 35, L06601, doi:10.1029/2007GL032971, 2008. 4325
- Tarantola, A. and Valette, B.: Generalized nonlinear inverse problems solved using the least squares criterion, *Rev. Geophys. Space Phys.*, 20, 219–232, 1982. 4342
- 20 Thierry, V., de Boisséson, E., and Mercier, H.: Interannual variability of the Subpolar Mode Water properties over the Reykjanes Ridge during 1990–2006, *J. Geophys. Res.*, 113, C04016, doi:10.1029/2007JC004443, 2008. 4325
- Toggweiler, J. R.: Carbon overconsumption, *Nature*, 363, 210–211, 1993. 4341
- 25 Treguier, A. M., Theetten, S., Chassignet, E. P., Penduff, T., Smith, R., Talley, L., Beismann, J. O., and Böning, C.: The North Atlantic Subpolar Gyre in Four High-Resolution Models, *J. Phys. Oceanogr.*, 35, 757–774, 2005. 4346, 4355
- van Aken, H. M., Femke de Jong, M., and Yashayaev, I.: Decadal and multi-decadal variability of labrador sea water in the north-western north atlantic ocean derived from tracer distributions: Heat budget, ventilation, and advection, *Deep Sea Res. I*, 58, 505–523, 2011. 4325
- 30 van Aken, H. M. and Becker, G.: Hydrography and through-flow in the north-eastern North Atlantic Ocean: The NANSEN project, *Prog. Oceanogr.*, 38, 297–346, 1996. 4340

Nutrients and oxygen budgets in the North-East Atlantic

G. Maze et al.

Title Page

Abstract

Introduction

Conclusions

References

Tables

Figures

⏪

⏩

◀

▶

Back

Close

Full Screen / Esc

Printer-friendly Version

Interactive Discussion



- van Aken, H. M. and de Boer, C.J. : On the synoptic hydrography of intermediate and deep water masses in the Iceland Basin, *Deep Sea Res. I*, 42, 165–189, 1995. 4340
- Yashayaev, I.: Hydrographic changes in the Labrador Sea, 1960–2005, *Prog. Oceanogr.*, 73, 242–276, 2007. 4325
- 5 Yashayaev, I., Bersch, M., and van Aken, H. M.: Spreading of the Labrador Sea Water to the Irminger and Iceland basins, *Geophys. Res. Lett.*, 34, L10602, doi:10.1029/2006GL028999, 2007. 4325
- 10 Yu, L., Jin, X., and Weller, R. A.: Multidecade Global Flux Datasets from the Objectively Analyzed Air-sea Fluxes (OAFux) Project: Latent and Sensible Heat Fluxes, Ocean Evaporation, and Related Surface Meteorological Variables, *Tech. rep.*, Woods Hole Oceanographic Institute, 2008. 4347, 4355

Table 1. A priori state estimates of parameters. Those adjusted by the optimization method are highlighted in bold face.

VARIABLE (UNIT)	ESTIMATE	±	ERROR	SOURCE
<i>Western Face transports (positive, eastward)</i>				
T_{nw}^{ρ} (10^9 kg s^{-1})	-13.3	±	1.5	OVIDE mean 2002,4,6
T_{sw}^{ρ} (10^9 kg s^{-1})	13.8	±	1.6	<i>Idem</i>
$T_{nw}^{\text{NO}_3}$ (kmol s^{-1})	-187.4	±	23.3	<i>Idem</i>
$T_{sw}^{\text{NO}_3}$ (kmol s^{-1})	199.1	±	28.5	<i>Idem</i>
$T_{nw}^{\text{PO}_4}$ (kmol s^{-1})	-12.2	±	1.5	<i>Idem</i>
$T_{sw}^{\text{PO}_4}$ (kmol s^{-1})	12.1	±	1.9	<i>Idem</i>
$T_{nw}^{\text{O}_2}$ (kmol s^{-1})	-4089	±	406	<i>Idem</i>
$T_{sw}^{\text{O}_2}$ (kmol s^{-1})	3208	±	429	<i>Idem</i>
$T_{nw}^{\text{O}_2}$ (kmol s^{-1})	-4387	±	460	<i>Idem</i>
$T_{sw}^{\text{O}_2}$ (kmol s^{-1})	3833	±	515	<i>Idem</i>
<i>Eastern Faces concentrations</i>				
ρ_{ne} (kg m^{-3})	1028.5			WOA09 annual climatology using the decomposition Eq. (B2)
ρ_{se} (kg m^{-3})	1028.7			<i>Idem</i>
$C_{ne}^{\text{NO}_3}$ ($\mu\text{mol kg}^{-1}$)	12.7			<i>Idem</i>
$C_{se}^{\text{NO}_3}$ ($\mu\text{mol kg}^{-1}$)	12.0			<i>Idem</i>
$C_{ne}^{\text{PO}_4}$ ($\mu\text{mol kg}^{-1}$)	0.9			<i>Idem</i>
$C_{se}^{\text{PO}_4}$ ($\mu\text{mol kg}^{-1}$)	0.8			<i>Idem</i>
$C_{ne}^{\text{O}_2}$ ($\mu\text{mol kg}^{-1}$)	332.3			<i>Idem</i>
$C_{se}^{\text{O}_2}$ ($\mu\text{mol kg}^{-1}$)	309.0			<i>Idem</i>
$C_{ne}^{\text{O}_2}$ ($\mu\text{mol kg}^{-1}$)	303.4			<i>Idem</i>
$C_{se}^{\text{O}_2}$ ($\mu\text{mol kg}^{-1}$)	285.5			<i>Idem</i>

Nutrients and oxygen budgets in the North-East Atlantic

G. Maze et al.

Title Page

Abstract

Introduction

Conclusions

References

Tables

Figures

◀

▶

◀

▶

Back

Close

Full Screen / Esc

Printer-friendly Version

Interactive Discussion



Nutrients and oxygen budgets in the North-East Atlantic

G. Maze et al.

[Title Page](#)
[Abstract](#)
[Introduction](#)
[Conclusions](#)
[References](#)
[Tables](#)
[Figures](#)
[⏪](#)
[⏩](#)
[◀](#)
[▶](#)
[Back](#)
[Close](#)
[Full Screen / Esc](#)
[Printer-friendly Version](#)
[Interactive Discussion](#)

Table 1. Continued.

VARIABLE (UNIT)	ESTIMATE	±	ERROR	SOURCE
<i>Reykjanes Ridge Face concentrations</i>				
ρ_{rr} (kg m ⁻³)	1030.7			WOA09 annual climatology
$C_{rr}^{NO_3}$ (μmol kg ⁻¹)	15.3			<i>Idem</i>
$C_{rr}^{PO_4}$ (μmol kg ⁻¹)	1.1			<i>Idem</i>
$C_{rr}^{O_2^s}$ (μmol kg ⁻¹)	302.1			<i>Idem</i>
$C_{rr}^{O_2}$ (μmol kg ⁻¹)	270.0			<i>Idem</i>
<i>Volume fluxes (positive, north or eastward)</i>				
F_{ne} (10 ⁶ m ³ s ⁻¹)	-4.3	±	2.2	IIC + EGC + DSOW
F_{se} (10 ⁶ m ³ s ⁻¹)	4.7	±	2.2	ISI + ISOW
F_{rr} (10 ⁶ m ³ s ⁻¹)	12.0	±	5.0	Treguier et al. (2005); Bower et al. (2002)
<i>Air-sea abiotic oxygen flux (positive, in-gassing)</i>				
J_n^a (kmol s ⁻¹)	100	±	200	Twice the annual thermal flux using surface WOA09 monthly climatology combined with OAflux heat fluxes (Yu et al., 2008)
J_s^a (kmol s ⁻¹)	160	±	320	<i>Idem</i>
<i>Biological source/sink terms of nitrate (positive, source)</i>				
B_n (kmol s ⁻¹)	16.0	±	32.0	Lee (2001) NCP estimates
B_s (kmol s ⁻¹)	75.2	±	150.4	<i>Idem</i>

Nutrients and oxygen budgets in the North-East Atlantic

G. Maze et al.

Table 2. Optimized mass transports across each of the box faces. Transports are positive north or eastward.

Face	Mass flux ($10^9 \text{ kg s}^{-1} \approx 1 \text{ Sv}$)
North/East (T_{ne}^{ρ})	-4.3 ± 0.4
North/West (T_{nw}^{ρ})	-13.7 ± 0.8
RR (T_{rr}^{ρ})	9.3 ± 0.7
South/East (T_{se}^{ρ})	4.8 ± 0.5
South/West (T_{sw}^{ρ})	14.1 ± 0.8

Title Page

Abstract

Introduction

Conclusions

References

Tables

Figures

◀

▶

◀

▶

Back

Close

Full Screen / Esc

Printer-friendly Version

Interactive Discussion

Nutrients and oxygen budgets in the North-East Atlantic

G. Maze et al.

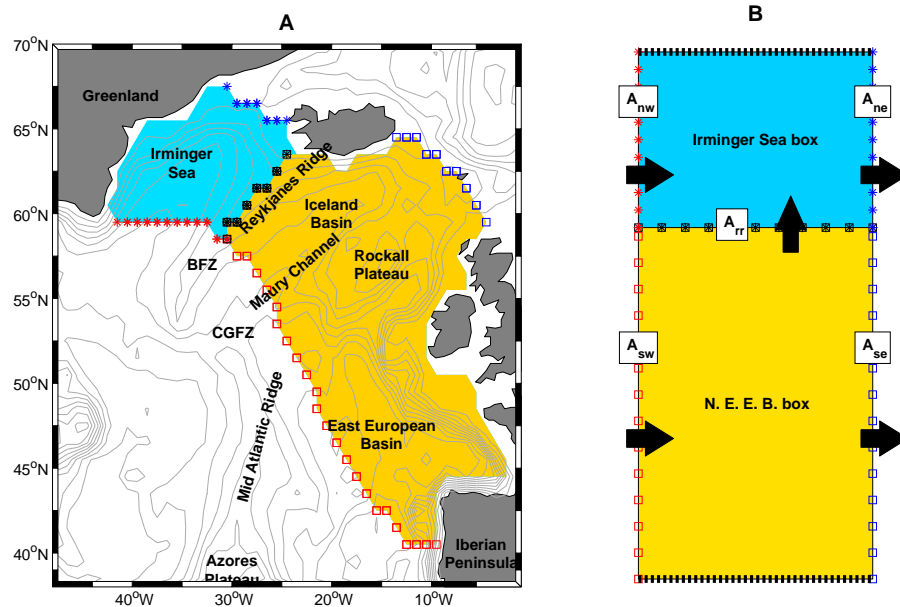


Fig. 1. (A) Localizations of the Irminger Sea (light blue shaded area) and North East European Basin (NEEB, yellow shaded area) box extend. Main geographic and topographic features are indicated. (B) The associated two box model simplified schematic. Black arrows indicate horizontal positive flux conventions. White background boxed labels indicate face naming conventions, here applied to face surfaces A . Blue/red star/square marks are drawn to help localize faces from panel (A) to (B).

Title Page

Abstract

Introduction

Conclusions

References

Tables

Figures

⏪

⏩

◀

▶

Back

Close

Full Screen / Esc

Printer-friendly Version

Interactive Discussion

Nutrients and oxygen budgets in the North-East Atlantic

G. Maze et al.

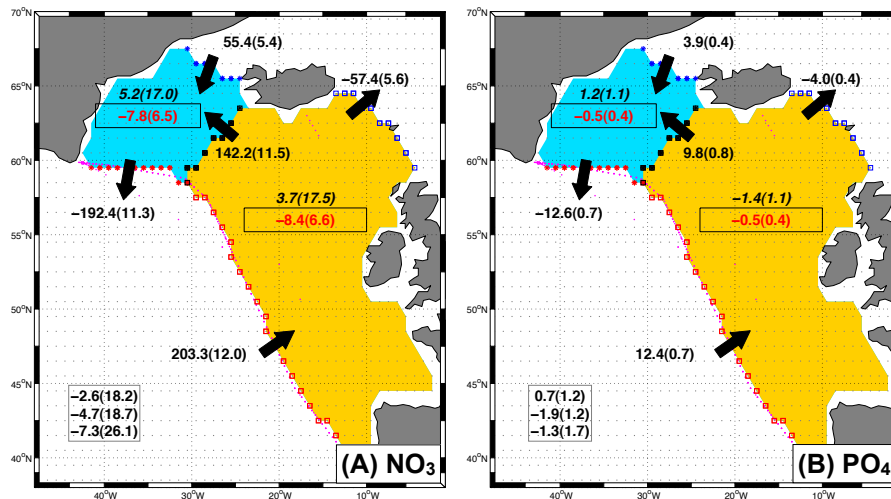


Fig. 2. (A) Nitrate and (B) Phosphate budget terms in kmol s^{-1} . Values are net for each box – i.e. negative value reducing concentration – except for the transport through RR which is plotted for the Irminger box (sign needs to be changed for the NEEB box). Black arrows indicate the transports directions. In the center of each box italic values are the transports divergence and framed red values are the biological net source/sink term. In the lower left corner are indicated the boxes and domain residuals. Values within parenthesis are error estimates.

Title Page

Abstract Introduction

Conclusions References

Tables Figures

◀ ▶

◀ ▶

Back Close

Full Screen / Esc

Printer-friendly Version

Interactive Discussion



Nutrients and oxygen budgets in the North-East Atlantic

G. Maze et al.

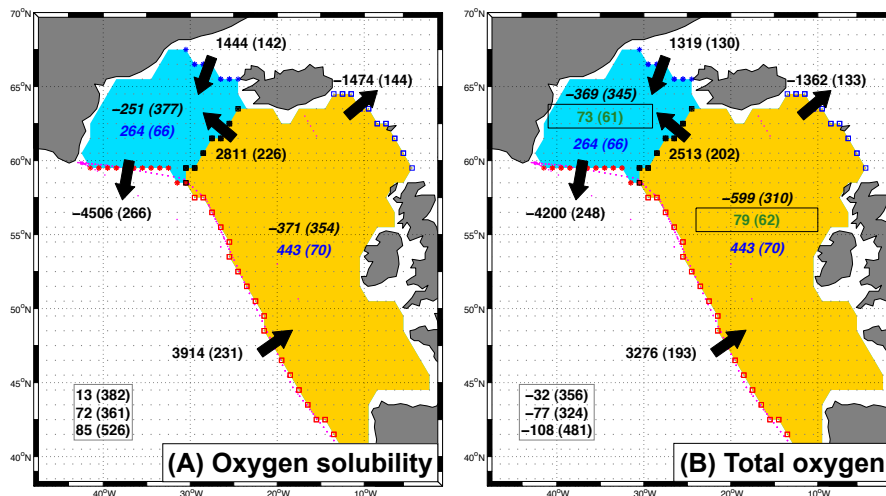


Fig. 3. (A) Oxygen solubility and (B) total oxygen budget terms in kmol s^{-1} . Values are net for each box – i.e. negative value reducing concentration – except for the transport through RR which is plotted for the Irminger box (sign needs to be changed for the NEEB box). Black arrows indicate the transports directions. In the center of each box italic values are the transports divergence, blue values are the air-sea abiotic oxygen flux (positive, downward) and framed green values are the biological net source/sink term for total oxygen. In the lower left corner are indicated the boxes and domain residuals. Values within parenthesis are error estimates.

Title Page

Abstract Introduction

Conclusions References

Tables Figures

⏪ ⏩

◀ ▶

Back Close

Full Screen / Esc

Printer-friendly Version

Interactive Discussion



Nutrients and oxygen budgets in the North-East Atlantic

G. Maze et al.

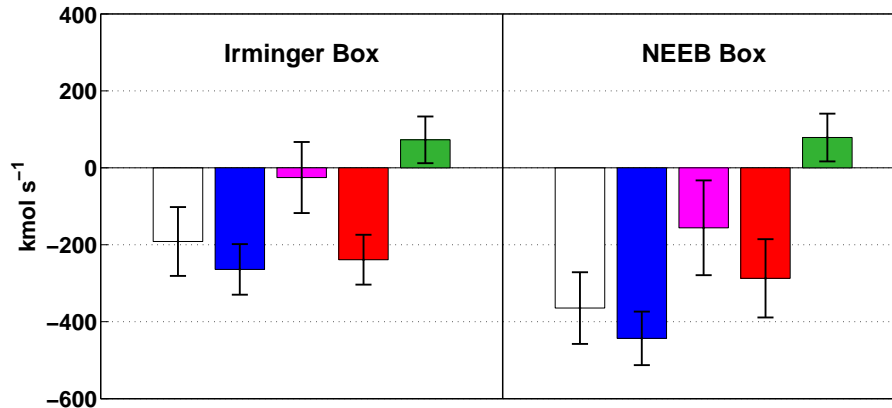


Fig. 4. Air-sea oxygen flux (kmol s^{-1}) partitioning for the Irminger (left) and NEEB (right) boxes. Note that here, negative fluxes are into the ocean (in-gassing). White: total flux, blue: abiotic flux, magenta: abiotic mixing flux, red: abiotic thermal flux and green: biotic flux. The error amplitude is represented on top of each bar.

Title Page

Abstract

Introduction

Conclusions

References

Tables

Figures

⏪

⏩

◀

▶

Back

Close

Full Screen / Esc

Printer-friendly Version

Interactive Discussion